

Supporting Information

Moisture-Induced Ionovoltaic Electricity Generation Using Lead Free 2-Dimensional $\text{Cs}_3\text{SbBiBr}_9$ Perovskite

Ashna K. Pramod ^{a, b}, Sudip K. Batabyal ^{a, b*}

^a Department of Physics, Amrita School of Physical Sciences, Coimbatore, Amrita Vishwa Vidyapeetham, India

^b Amrita Center for Industrial Research & Innovation (ACIRI), Amrita School of Engineering, Coimbatore, Amrita Vishwa Vidyapeetham, India.

Corresponding Author Email: * s_batabyal@cb.amrita.edu

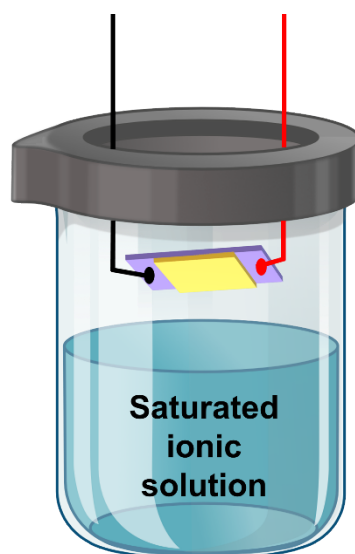


Fig.S1: Schematic representation of $\text{Cs}_3\text{SbBiBr}_9$ ionovoltaic device measurement setup

Table 1. Calculated lattice parameters of the lead-free perovskite powders $\text{Cs}_3\text{Sb}_2\text{Br}_9$, $\text{Cs}_3\text{Bi}_2\text{Br}_9$ and $\text{Cs}_3\text{SbBiBr}_9$

Perovskite	Lattice parameters					
	Theoretical (Å)			Experimental (Å)		
	a	b	c	a	b	c
$\text{Cs}_3\text{Bi}_2\text{Br}_9$	7.97	7.97	9.86	8.03	8.03	9.67
$\text{Cs}_3\text{Sb}_2\text{Br}_9$	7.93	7.93	9.71	7.92	7.92	9.74

$\text{Cs}_3\text{SbBiBr}_9$	7.93	7.93	9.71	7.91	7.90	9.73
------------------------------	------	------	------	------	------	------

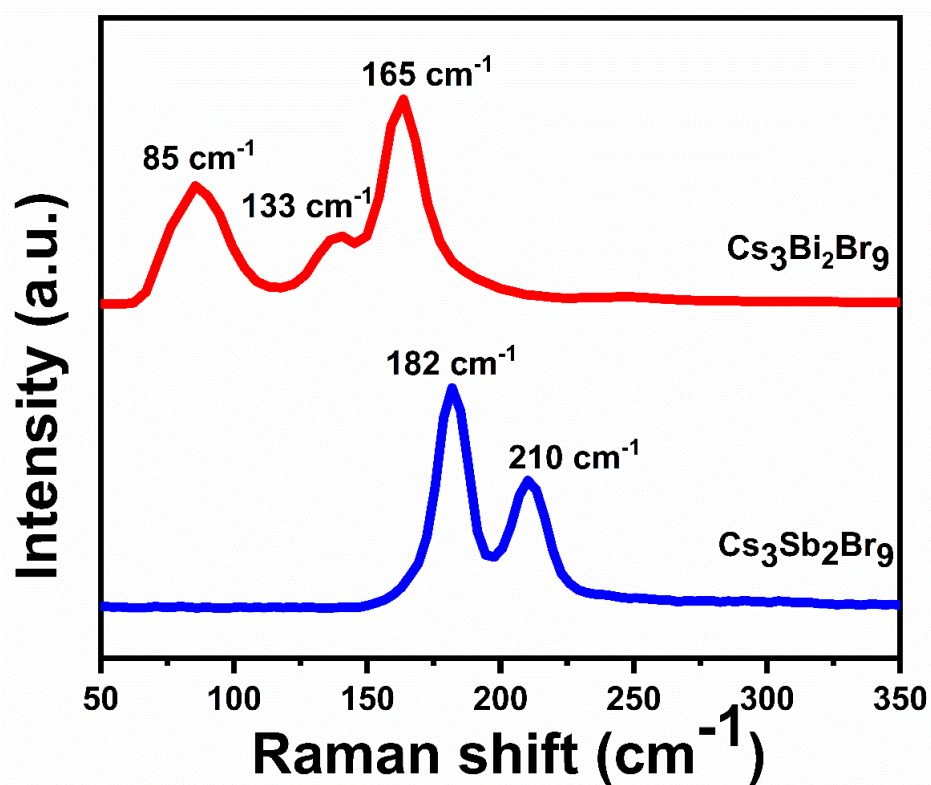


Fig.S2: Raman spectra of $\text{Cs}_3\text{Sb}_2\text{Br}_9$ and $\text{Cs}_3\text{Bi}_2\text{Br}_9$

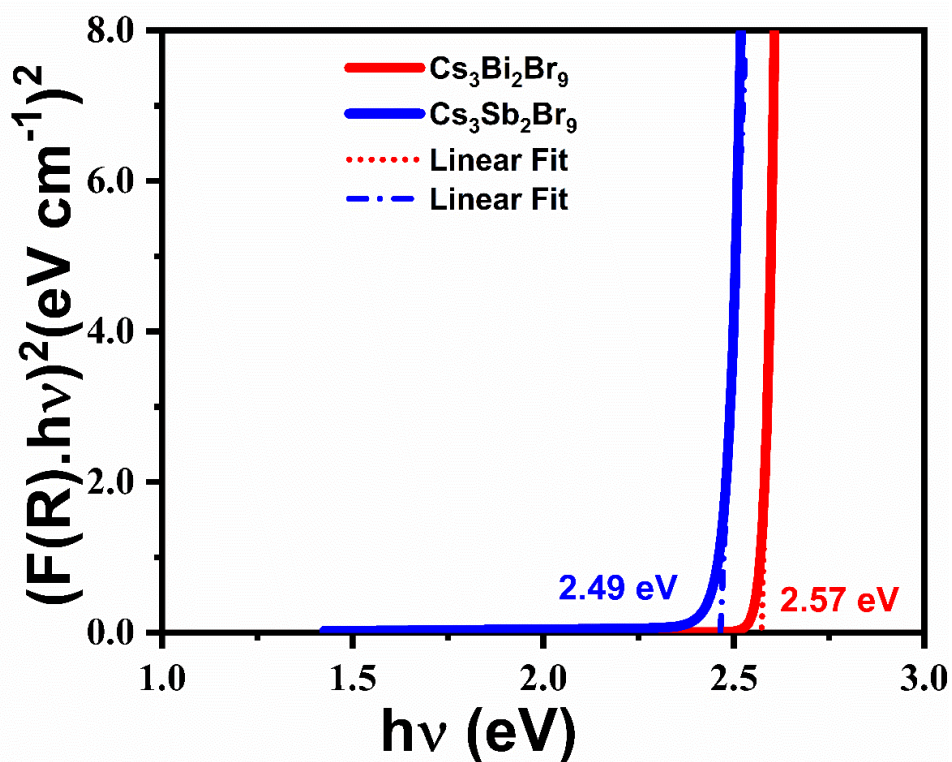


Fig.S3: Band gap of $\text{Cs}_3\text{Sb}_2\text{Br}_9$ and $\text{Cs}_3\text{Bi}_2\text{Br}_9$

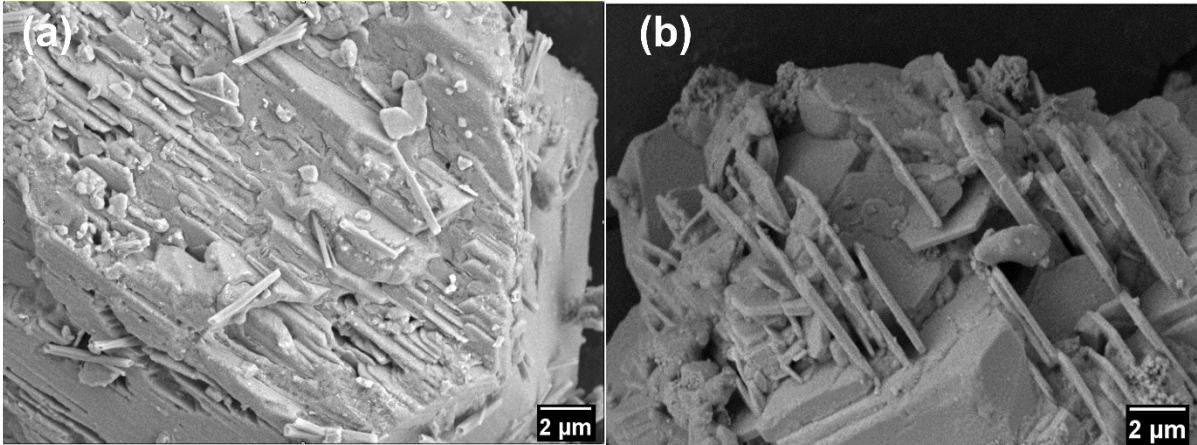


Fig.S4: SEM image of pristine $\text{Cs}_3\text{SbBiBr}_9$ thick blocks with layered structure

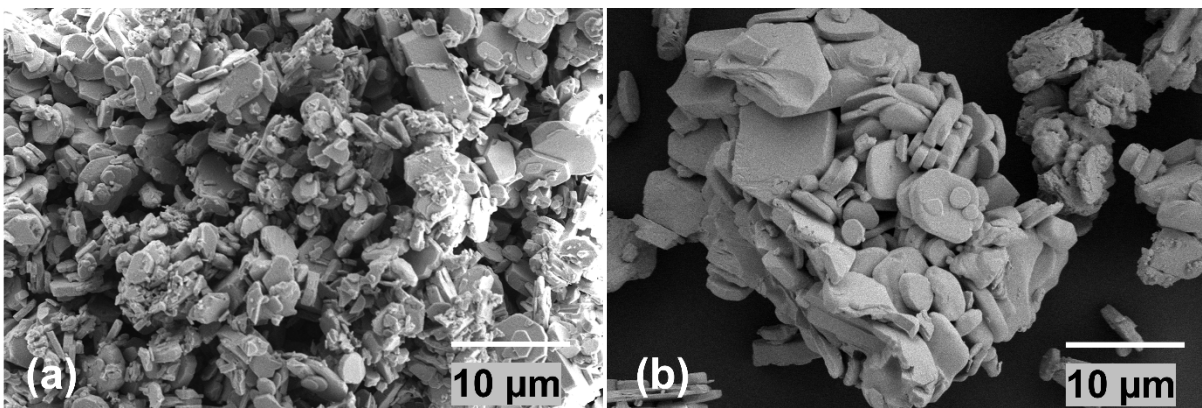


Fig.S5: (a) SEM image of lead -free perovskite $\text{Cs}_3\text{Sb}_2\text{Br}_9$ powder; (b) SEM image of lead -free perovskite $\text{Cs}_3\text{Bi}_2\text{Br}_9$ powder hexagonal morphology

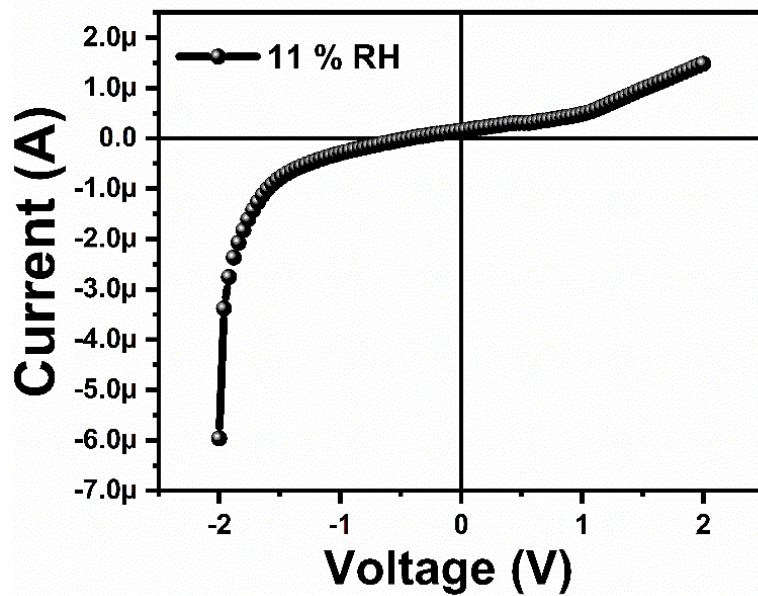


Fig.S6: Zoomed in view of the I-V curve at 11 % RH

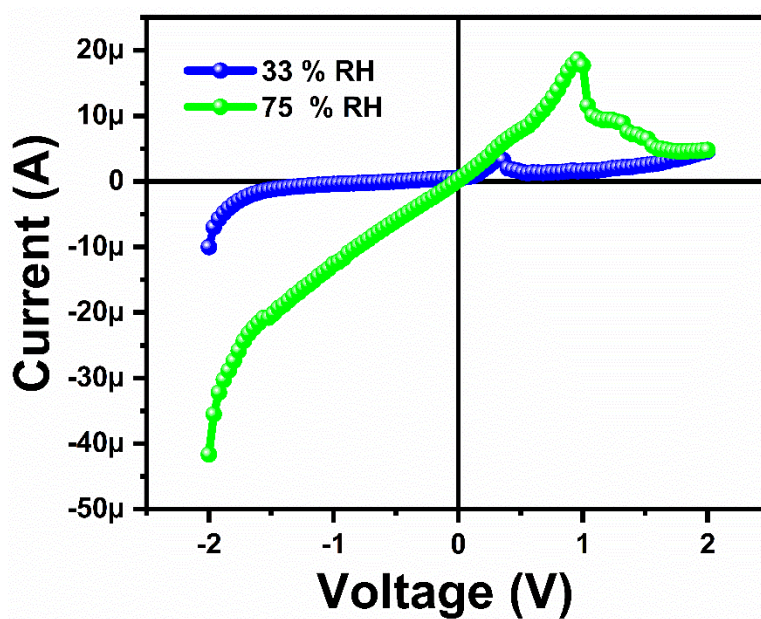


Fig.S7: Current-voltage curves measured at 33 % and 75 % RH

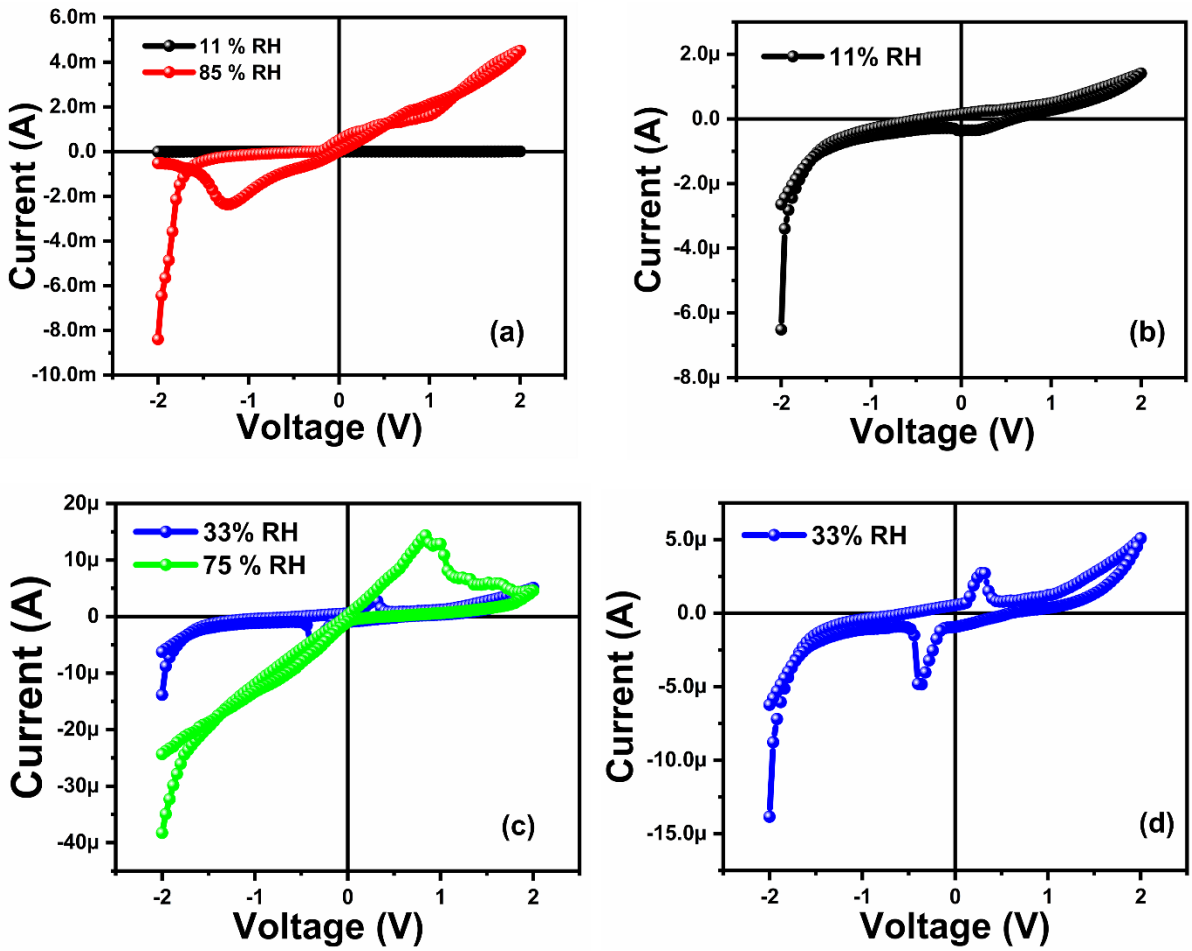


Fig.S8: I-V loop demonstrating energy storage behavior;(a) I-V loop at 11and 85% RH;
 (b) Zoomed in view of the I-V loop curve at 11 % RH;(c) I-V loop at 33 and 75% RH;
 (b) Zoomed in view of the I-V loop curve at 33 % RH

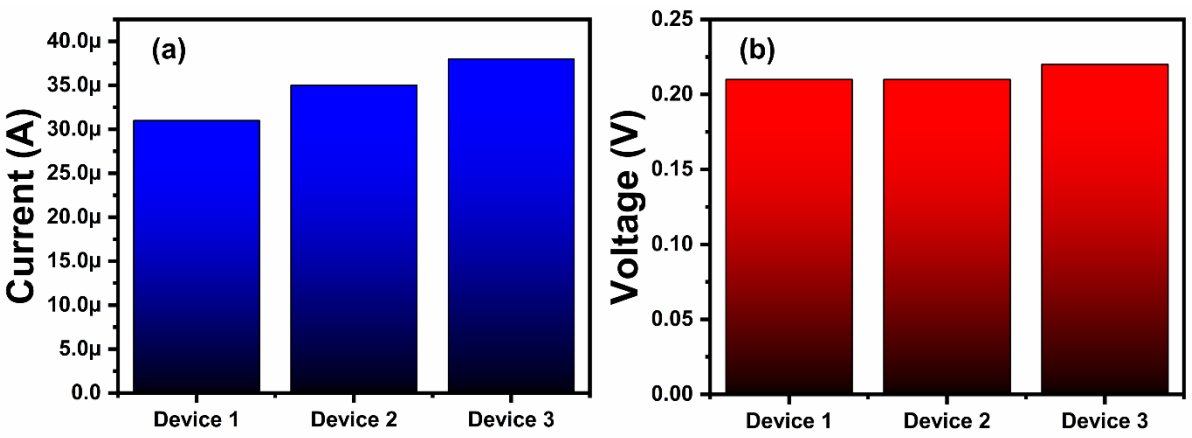


Fig.S9: Statistical data for three ionovoltaic devices

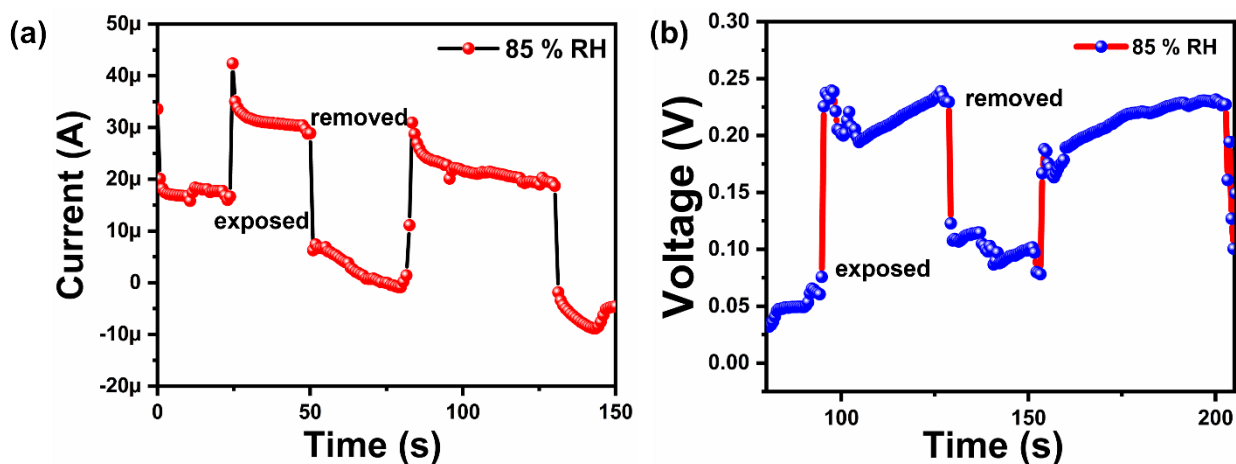


Fig.S10: (a) Current output was measured during sequential exposure and removal from the 85% RH;(b) Voltage output was measured during sequential exposure and removal from the 85% RH

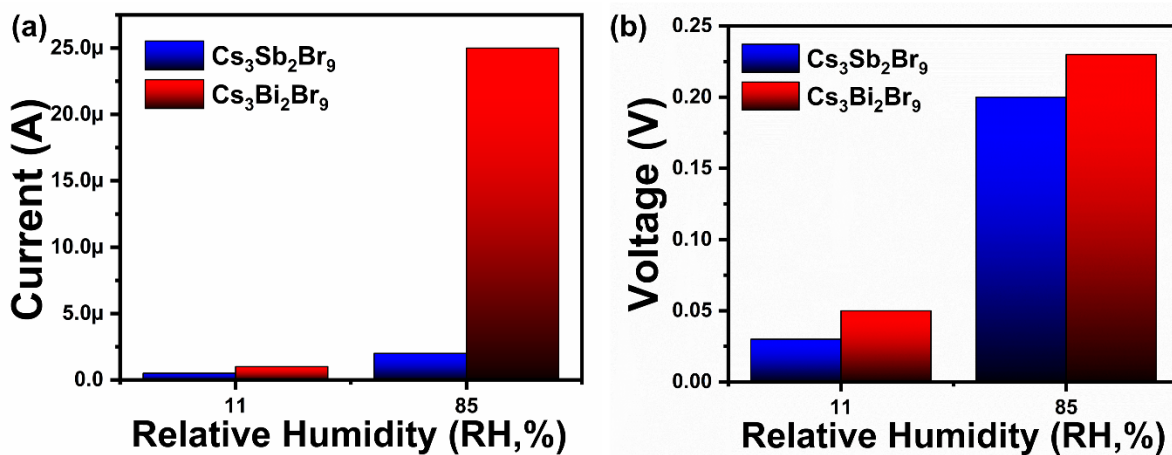


Fig.S11: I-t and V-t measurement of the $\text{Cs}_3\text{Sb}_2\text{Br}_9$ and $\text{Cs}_3\text{Bi}_2\text{Br}_9$ ionovoltaic device exposed to varying level of relative humidity

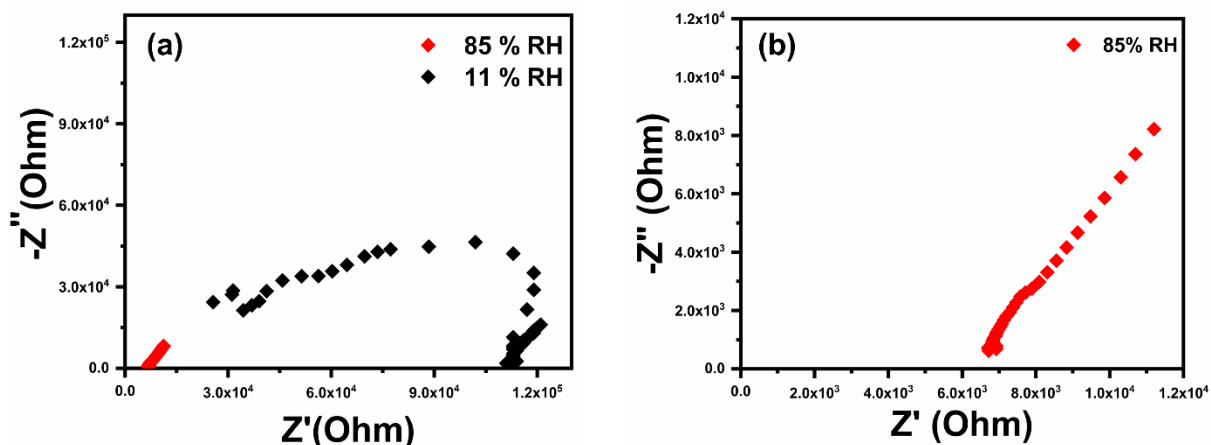


Fig.S12: (a) presents the Nyquist plots obtained for the ionovoltaic device when subjected to relative humidity level of 11% and 85%; (b) Zoomed image of 85 % RH

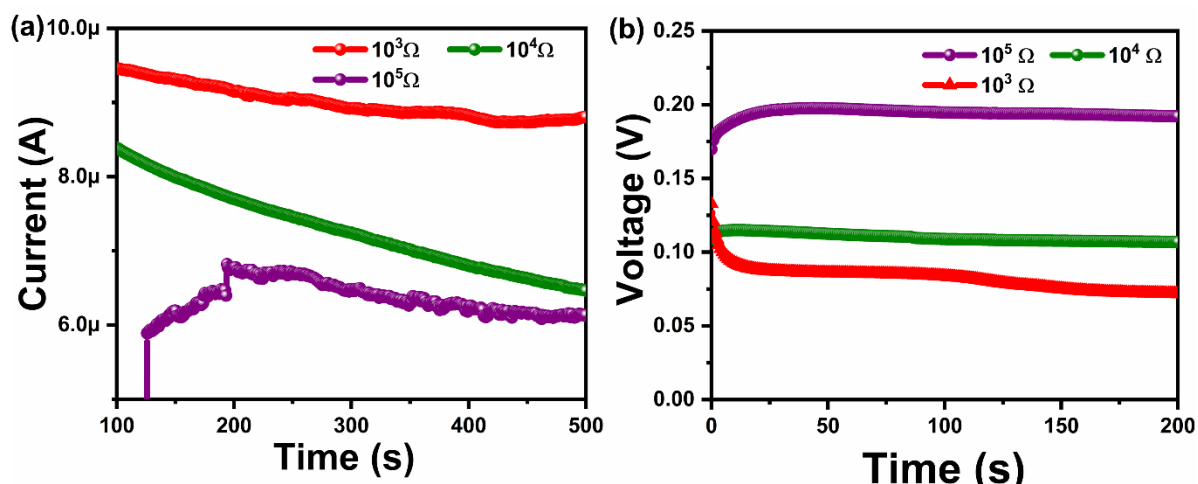


Fig.S13: (a) I-t measurement showing varying resistances; (b) V-t measurement illustrating varying resistances

Table 2: Power density calculation at 85% RH with varying resistance

Resistance	I_{sc} (A)	V_{oc} (V)	Area ($1.5 \text{ cm} \times 0.2 \text{ cm} = 0.3 \text{ cm}^2$)	Current density $J=I/A$ ($\mu\text{A}/\text{cm}^2$)	Power density ($\mu\text{W}/\text{cm}^2$)
10^3	9.5×10^{-6}	0.08	0.3	31	2.53
10^4	6.3×10^{-6}	0.108	0.3	21	2.31
10^5	6.1×10^{-6}	0.2	0.3	20	4.09

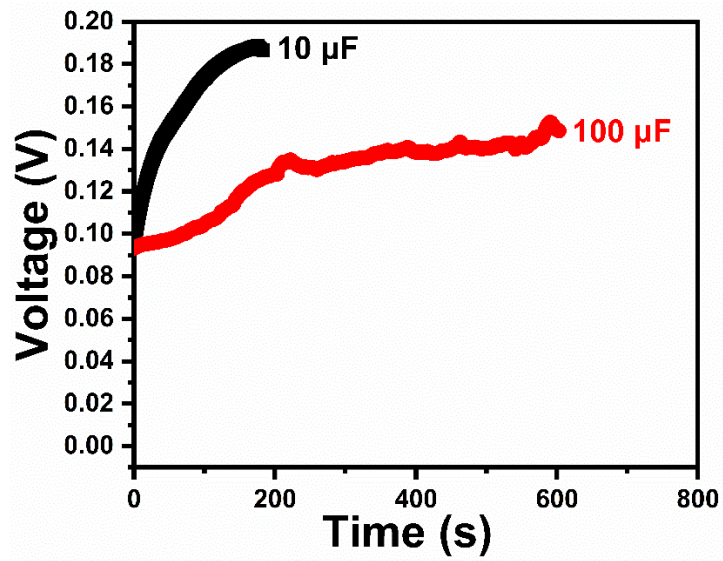


Fig.S14: Illustrates the charging behavior of capacitors with capacitances of 10 µF and 100 µF using single ionovoltaic devices in an environment with 75% RH